

# Equations of state for neutron matter derived from ladder diagrams and its extrapolation from basic principles

J. A. OLLER

Departamento de Física  
Universidad de Murcia

In collaboration with J.M. Alarcón and E. Lope Oter

Alarcón, JAO, PRC106(2022), AP107(2022)  
Lope Oter *et al.*, JPG46(2019)

New Frontiers in Strong Gravity 2024  
Banasque Science Center



- 1 Introduction
- 2 In-medium many-body
- 3  $\mathcal{E}_{\mathcal{L}}$  in the ladder approximation
- 4 Partial waves
- 5 Explicit solution: Contact-interaction potential
- 6 Applications:  $S$ -waves
- 7 Applications: Neutron matter
- 8 Applications: Symmetric Nuclear Matter
- 9 Conclusions

# Introduction

$$\text{Energy/fermion} = E/A = \bar{\mathcal{E}}$$

- $E/A$  in a many-body system formed by fermions is a fundamental Basic Problem
- Particle-Nuclear physics: Symmetric nuclear matter, neutron matter, neutron stars, quark-gluon plasma, etc
- Condensed matter: Cooper pairs, BCS, Hubbard Hamiltonian (contact constant interaction), BEC, ...
- AMO: Trapped ultra-cold atomic gases, unitary limit ( $a_s \rightarrow \infty$ ), BEC–BCS crossover, ...

## Master Equation for the Energy Density $\mathcal{E}_{\mathcal{L}}$

$$\begin{aligned}\mathcal{E}_{\mathcal{L}} &= \frac{i}{2} \text{Tr} \left( \sum_{d=1}^{\infty} \frac{(t_m L_d)^d}{d} \right) = -\frac{i}{2} \text{Tr} \log [I - t_m L_d] \\ &= -\frac{i}{2} \text{Tr} \log e^{2iV_{\text{eff}}} = \text{Tr} V_{\text{eff}}\end{aligned}$$

- The trace is taken in the three-momentum, isospin and spin spaces
- $t_m$  is the in-medium  $T$  matrix. Calculated from the vacuum  $T$  matrix,  $t_V$ .

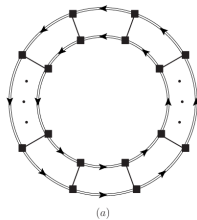
$$L_d(p, \mathbf{a}) = \begin{array}{c} \text{Diagram: A ladder diagram with two vertical rungs and two horizontal legs. The top horizontal leg has an arrow pointing right and is labeled } a+k. \text{ The bottom horizontal leg has an arrow pointing right and is labeled } a-k. \text{ The left vertical rung has an arrow pointing up and is labeled } p. \text{ The right vertical rung has an arrow pointing up and is labeled } p. \end{array} = i \frac{mp}{8\pi^2} \int d\hat{k} \theta(k_F - |\mathbf{a} + p\hat{k}|) \theta(k_F - |\mathbf{a} - p\hat{k}|) |p\hat{k}, \sigma_1, \sigma_2\rangle \langle p\hat{k}, \sigma_1, \sigma_2|$$

(a)

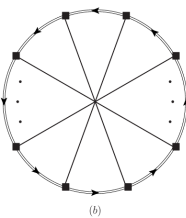
# Resummation of ladder diagrams

$t_m \equiv$  Squares joined by inward lines

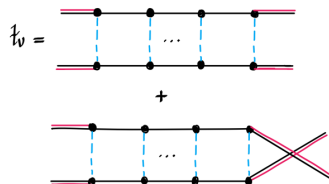
$t_V$  arises by expanding the  $\Gamma$  vertices



Hartree



Fock



It is an interesting combinatorial problem to get  $\mathcal{E}_{\mathcal{L}} = -\frac{i}{2} \text{Tr} \log [I - t_m L_d]$

Alarcón, JAO, Ann. Phys. 437, 168741 (2022)

- The reformulation of many-body field-theory in [JAO, PRC 65, 025204 \(2002\)](#) drives to an adequate arrangement of the diagrams and solves their resummation

- For arbitrary vacuum fermion-fermion interaction
- For arbitrary regularization method

## In-medium many-body formalism: One-nucleon sector

### Vacuum-vacuum transition amplitude

$$e^{i\mathcal{L}[J]} = \langle 0_{\text{out}} | 0_{\text{in}} \rangle_J$$

In QCD/ChPT, typically  $J = \{v, a, s, p\}$

$$\mathcal{L}_{\text{ext}} = \mathcal{L}_{\text{QCD}}^0 + \bar{q} \gamma^\mu (v_\mu + \gamma_5 a_\mu) q - \bar{q} (s - ip) q$$

Gasser,Sainio,Svarc,NPB307(1988)

### One-nucleon-one-nucleon transition amplitude

$$\mathcal{F}(\mathbf{p}', \mathbf{p})[J] = \langle \mathbf{p}'_{\text{out}} | \mathbf{p}_{\text{in}} \rangle_J$$

$$\mathcal{L}_{\pi N} = -\bar{\psi} D \psi$$

$$\mathcal{L} = \mathcal{L}_{\pi\pi} + \mathcal{L}_{\pi N} + \bar{\eta} \psi + \bar{\psi} \eta$$

$\eta$  is a fermionic source

## In-medium many-body formalism

JAO, PRC65(2002): Similar ideas to many-body field theory:

$$|\Omega\rangle_{\text{in}; \text{out}} = \prod_n^N a(\mathbf{p}_n \sigma_n)_{\text{in}; \text{out}}^\dagger |\text{vacuum}\rangle$$

$$\mathcal{L} = \underbrace{\mathcal{L}_\phi}_{\text{Pure Mesonic}} + \underbrace{\bar{\psi}(D_0 - V)\psi}_{\text{Bilinear}} + \bar{\eta}\psi + \bar{\psi}\eta$$

Mesons exchanged:

Light, Heavier ones ( $M_H \rightarrow \infty$  contact interactions)

$$e^{i\mathcal{L}[J]} = \langle \Omega_{\text{out}} | \Omega_{\text{in}} \rangle_J$$

Generating Functional: Fermions in the Fermi sea are integrated out

$$e^{i\mathcal{L}[J]} = \int [dU] \exp \left\{ i \int dx \mathcal{L}_\phi + \text{Tr} \int \frac{d^3 p \mathbf{n}(\mathbf{p})}{(2\pi)^3} \int d^3 x d^3 y e^{-i\mathbf{p}\mathbf{x}} \log \mathcal{F}(\mathbf{x}, \mathbf{y}) e^{i\mathbf{p}\mathbf{y}} \right\}$$

Tr Trace over discrete internal indices

$$n(p) = \begin{pmatrix} \theta(k_F - |\mathbf{p}|) & 0 \\ 0 & \theta(k_F - |\mathbf{p}|) \end{pmatrix}$$

$$\mathcal{F}(\mathbf{x}, \mathbf{y})_{\alpha\beta} = \delta(\mathbf{x} - \mathbf{y}) \delta_{\alpha\beta}$$

$$- i \int dt \int dt' e^{iH_0 t} \gamma^0 [\mathcal{V}[\mathcal{I} - D_0^{-1} \mathcal{V}]^{-1}] (\mathbf{k}, \mathbf{y})_{\alpha\beta} e^{-iH_0 t'}$$

$$\Gamma = \text{(-iV)} + \text{(-iV)} \xrightarrow{\text{iD}_0^{-1}} \text{(-iV)} + \text{(-iV)} \xrightarrow{\text{iD}_0^{-1}} \text{(-iV)} \xrightarrow{\text{iD}_0^{-1}} \text{(-iV)} + \dots$$

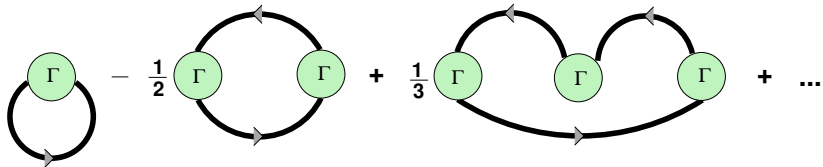
$\Gamma$  is a non-local vertex: Geometric series

**Vacuum fermion propagator:**  $D_0^{-1} = \frac{i\delta_{\sigma\sigma'}}{(p^0 - \mathbf{p}^2/(2m) + i\epsilon)}$

# Perturbative Expansion

- Series expansion of  
 $\log(1 + \epsilon) = -\sum (-1)^d \epsilon^d / d$
- $d$  is the number of Fermi-sea insertions
- Each of them provides an extra  $(-)$  sign
- Notice the symmetry factor  
 $1/d$

$$e^{i\mathcal{L}[J]} = \int [dU] \exp \left[ i \int dx \mathcal{L}_\phi \right.$$
$$\left. - i \int \frac{d\mathbf{p}}{(2\pi)^3} \int \text{Tr} \left( V[I - D_0^{-1}V]^{-1} |_{(x,y)} n(\mathbf{p}) \right) dx dy e^{ip(x-y)} \right.$$
$$\left. - \frac{1}{2} \int \frac{d\mathbf{p}}{(2\pi)^3} \int \frac{d\mathbf{q}}{(2\pi)^3} \int \text{Tr} e^{ip(x-y)} e^{-iq(x'-y')} dx dx' dy dy' \right.$$
$$\left. \times \left( V[I - D_0^{-1}V]^{-1} |_{(x,x')} n(\mathbf{q}) V[I - D_0^{-1}V]^{-1} |_{(y',y)} n(\mathbf{p}) \right) + \dots \right]$$



In-medium Generalized Vertices (IGV's)

# Integral equation (IE) for $t_m(\mathbf{a})$

- $\mathbf{a} = \frac{1}{2}(\mathbf{k}_1 + \mathbf{k}_2)$ ,  $\mathbf{p} = \frac{1}{2}(\mathbf{k}_1 - \mathbf{k}_2)$

Vacuum intermediate states  $G(p)$

$$G(p) = \text{Diagram: A square loop with two vertical sides and two horizontal sides. The top horizontal side has an arrow pointing right labeled 'a+k'. The bottom horizontal side has an arrow pointing left labeled 'a-k'. The left vertical side has an arrow pointing down labeled 'a-k'. The right vertical side has an arrow pointing up labeled 'a+k'.$$

$$= -m \int \frac{d^3 k}{(2\pi)^3} \frac{|p\hat{\mathbf{k}}, \sigma_1, \sigma_2\rangle \langle p\hat{\mathbf{k}}, \sigma_1, \sigma_2|}{k^2 - p^2 - i\epsilon}$$

Vacuum  $T$  matrix  $t_V$        $t_V = V - V G(p) t_V$

Mixed intermediate states  $L_m(p, \mathbf{a})$

$$L_m(p, \mathbf{a}) = \text{Diagram: Two square loops stacked vertically. The top loop has an arrow pointing right labeled 'a+k' on the top and left sides, and an arrow pointing left labeled 'a-k' on the bottom. The bottom loop has an arrow pointing right labeled 'a+k' on the top and left sides, and an arrow pointing left labeled 'a-k' on the bottom. Below the bottom loop is the label '(b)'.$$

$$+ \text{Diagram: Two square loops stacked vertically. The top loop has an arrow pointing right labeled 'a+k' on the top and left sides, and an arrow pointing left labeled 'a-k' on the bottom. The bottom loop has an arrow pointing right labeled 'a+k' on the top and left sides, and an arrow pointing left labeled 'a-k' on the bottom. Below the bottom loop is the label '(b)'.$$

$$= -m \int \frac{d^3 k}{(2\pi)^3} \frac{\theta(k_F - |\mathbf{a} + \mathbf{k}|) + \theta(k_F - |\mathbf{a} - \mathbf{k}|)}{k^2 - p^2 - i\epsilon} |p\hat{\mathbf{k}}, \sigma_1, \sigma_2\rangle \langle p\hat{\mathbf{k}}, \sigma_1, \sigma_2|$$

In-medium  $T$  matrix  $t_m(\mathbf{a})$

- $|\mathbf{k}|$  is bounded in  $L_m$  and  $L_d$
- No extra divergences stem from  $L_m$

$$t_m(\mathbf{a}) = t_V + t_V L_m(p, \mathbf{a}) t_m(\mathbf{a})$$

$$t_m(\mathbf{a}) = V + V (G(p) - L_m(p, \mathbf{a})) t_m(\mathbf{a})$$

The formula for  $\mathcal{E}_{\mathcal{L}}$  gives real values

$$\begin{aligned}\mathcal{E}_{\mathcal{L}} &= -\frac{i}{2} \text{Tr} \log [I - t_m L_d] & t_m(\mathbf{a})^{-1} &= V^{-1} + G - L_m(p, \mathbf{a}) \\ &= -\frac{i}{2} \text{Tr} \log [\mathbf{t}_m(\mathbf{t}_m^{-1} - i \mathbf{L}_d)] & \mathcal{E}_{\mathcal{L}} &= -\frac{i}{2} \text{Tr} \log [\mathbf{A}^{-1} \mathbf{B}] \\ && \mathbf{A} &= V^{-1} + G - L_m(p, \mathbf{a}) \\ && \mathbf{B} &= V^{-1} + G - L_m(p, \mathbf{a}) - L_d(p, \mathbf{a})\end{aligned}$$

Within the Fermi seas, where the Tr is taken:  $A = B^\dagger$

$I - t_m L_d$  is a unitary matrix

We diagonalize it and sum over its eigenvalues for calculating

$$\text{Tr} \log [I - t_m L_d]$$

## Partial waves

- Low energies: One typically characterizes  $t_V$  by summing over partial-wave amplitudes (PWAs)
- But in the medium the scattering depends on the total three-momentum ( $2\mathbf{a}$ )

### PWAs mix

Notice,

$$\int d\hat{\mathbf{k}} Y_\ell^m(\hat{\mathbf{k}}) Y_{\ell'}^{m'}(\hat{\mathbf{k}})^* \theta(\xi - |a\hat{\mathbf{z}} \pm \hat{\mathbf{k}}|) \neq 0$$

Transformation under a rotation  $R$

$$L_m(p, R\mathbf{a}) = RL_m(p, \mathbf{a})R^\dagger$$

$$L_d(p, R\mathbf{a}) = RL_d(p, \mathbf{a})R^\dagger$$

$$t_V = Rt_VR^\dagger$$

$$t_m(R\mathbf{a}) = Rt_m(\mathbf{a})R^\dagger$$

$$\chi(S\ell I) = \frac{1 - (-1)^{\ell+S+I}}{\sqrt{2}}, \quad \ell + S + I = \text{odd}$$

$$\mathcal{E}_{\mathcal{L}} = -\frac{2i}{m\pi^3} \sum_{\substack{J, \mu, \ell \\ S, I, i_3}} \chi(S\ell I)^2 \int_0^\infty pdp \int_0^\infty a^2 da \langle J\mu\ell S i_3 p | \log [I - t_m(a\hat{z}) L_d(p, a\hat{z})] | J\mu\ell S i_3 p \rangle$$

Mixing of  $J$ 's for  $a\hat{z}$ . IE for  $t_m(a\hat{z})$  in PWAs [v], [ $t_V$ ], [ $t_m$ ] matrices in the space of coupled PWAs

$$[t_m(a\hat{z})](p', p) = [t_V](p', p)$$

$$+ \frac{m}{(2\pi)^2} \int_0^\infty \frac{k^2 dk}{k^2 - p^2 - i\epsilon} [t_V](p', k) \cdot \mathcal{B} \cdot [t_m(a\hat{z})](k, p)$$

$$[t_V](p', k)_{J'\ell', J_2\ell_2} = \delta_{J'J_2} \langle J'\mu\ell' Sp' | t_V | J_2\mu\ell_2 Sk \rangle ,$$

$$\begin{aligned} \mathcal{B}_{J_2\mu\ell_2, J_1\mu\ell_1} &= -2\chi(S\ell_2)\chi(S\ell_1) \sum_{m_3 s_3} (m_3 s_3 \mu | \ell_2 S J_2) (m_3 s_3 \mu | \ell_1 S J_1) \\ &\times \int d\hat{\mathbf{k}} Y_{\ell_2}^{m_3}(\hat{\mathbf{k}})^* Y_{\ell_1}^{m_3}(\hat{\mathbf{k}}) \theta(k_F - |\mathbf{k} - a\hat{z}|) . \end{aligned}$$

# Explicit solution: Contact-interaction potential JAO'18

$n$  coupled PWAs

$$v_{\alpha\beta}(k, p) = k^{\ell_\alpha} p^{\ell_\beta} \sum_{i,j=1}^N v_{\alpha\beta;ij} k^{2(i-1)} p^{2(j-1)}$$

$$v_{\alpha\beta}(k, p) = [k_\alpha]^T \cdot [v] \cdot [p_\beta]$$

$$[v] = \begin{pmatrix} [v_{11}] & [v_{12}] & \dots & [v_{1n}] \\ [v_{21}] & [v_{22}] & \dots & [v_{2n}] \\ \dots & \dots & \dots & \dots \\ [v_{n1}] & [v_{n2}] & \dots & [v_{nn}] \end{pmatrix}$$

$$[k_\alpha]^T = (\underbrace{0, \dots, 0}_{N(\alpha-1) \text{ places}}, k^{\ell_\alpha}, k^{\ell_\alpha+2}, \dots, k^{\ell_\alpha+2(N-1)}, 0, \dots, 0)$$

$$t_V(k, p) = [k_\alpha]^T \cdot [\hat{t}_V(p)] \cdot [p_\beta],$$

$[\hat{t}_V(p)]$  is given by the *algebraic* equation

$$[\hat{t}_V(p)] = [v] - [v] \cdot [\mathcal{G}(p)] \cdot [\hat{t}_V(p)]$$

$$[\hat{t}_V(p)] = (I + [v] \cdot [\mathcal{G}(p)])^{-1} \cdot [v]$$

$$[\mathcal{G}(p)_{\alpha\beta}] = -\frac{m}{(2\pi)^2} \int_0^\infty \frac{k^2 dk}{k^2 - p^2 - i\epsilon} [k_\alpha][k_\beta]^T$$

Divergent integrals [General cutoff regularization van Kolck'99]

$$\mathcal{L}_n = -\frac{m}{2\pi^2} \int_0^\infty dk k^{n-1} = \theta_n \Lambda^n ,$$

$\theta_n$  depends on the scheme (DR is  $\theta_n = 0$ )

**Renormalization:** Matching with the  
Effective Range Expansion (ERE) in vacuum ( $k_F = 0$ )

$$\frac{4\pi}{m} (p^\ell) t_V(p, p)^{-1}(p^\ell) + i(p^\ell)^2(p) = -(a)^{-1} + \frac{1}{2}(r)p^2 + \sum_{i=2}^M (v_\ell^{(2i)}) p^{2i}$$

( $a$ ), ( $r$ ) and ( $v_\ell^{(2i)}$ ):  $n \times n$  matrices ,  $(p)^\ell = \text{diag}(p^{\ell_1}, \dots, p^{\ell_n})$

Once renormalized with  $\theta_n \neq 0$  and  $\Lambda \rightarrow \infty$ , the solution is

$$t_V(k, q) = \frac{4\pi}{m} (k)^\ell \tau(p) q^\ell , \text{ Off-shell}$$

$$\tau(p)^{-1} = -(a)^{-1} + \frac{1}{2}(r)p^2 + \sum_{i=2}^M (v_\ell^{(2i)}) p^{2i} - i(p^\ell)^2(p) , \text{ on-shell}$$

**Reason:**  $p, k \leq k_F$  ( $k_F/\Lambda \rightarrow 0$ )

Uncoupled:  $\tau(p) = \frac{1}{p \cot \delta}$       We can take  $M \rightarrow \infty$

Coupled:  $\tau(p) = (p)^{-\ell} \frac{1}{2ip} (S_{JS} - 1) (p)^{-\ell}$  .

$$t_V(q, q') = \frac{(qq')^\ell}{p^{2\ell+1} \cot \delta_\ell - ip^{2\ell+1}}$$

$$t_m(q, q') = \frac{(qq')^\ell}{p^{2\ell+1} \cot \delta_\ell - ip^{2\ell+1} - q'^\ell L_m q'^\ell}$$

# Applications: $S$ waves, $v(k, p) = c_0$

Alarcón, JAO, Ann. Phys. 437, 168741 (2022)

$$\tau_m(p) = \left( -\frac{1}{a_0} - ip + \mathcal{G}_m(p) \right)^{-1}$$

$$\mathcal{E}_{\mathcal{L}} = \frac{8k_F^5}{m\pi^3} \int_0^1 s^2 ds \int_0^{\sqrt{1-s^2}} \kappa d\kappa \arctan \left( \frac{a_0 k_F I}{1 - a_0 k_F R / \pi} \right)$$

$$s = a/k_F, \kappa = p/k_F, R + i\pi I = (\mathcal{G}_m - ip)\pi/k_F \quad \text{Kaiser'11}$$

$$\bar{\mathcal{E}} = \frac{3k_F^2}{10m} \left\{ \xi + \frac{\zeta}{a_0 k_F} - \frac{5\nu}{3(a_0 k_F)^2} + \dots \right\}$$

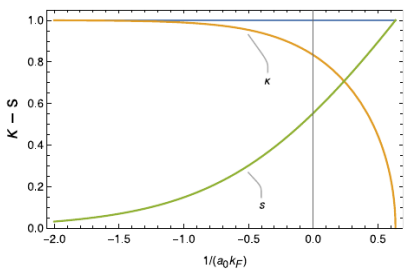
Bertsch parameter

$$\xi = 1 - \frac{80}{\pi} \int_0^1 ds s^2 \int_0^{\sqrt{1-s^2}} d\kappa \kappa \arctan \left( \frac{\pi I}{R} \right) = 0.5066.$$

- The experimental actual value in the superfluid phase is  $\xi = 0.370(5)(8)$  Ku et al., Science 335 (2012) 563
- The experimental value of  $\xi$  for normal matter at the unitary limit is  $\xi \approx 0.45$  Navon et al, Science 328 (2010) 729

# In-medium poles in the $S$ -wave amplitude at the Fermi surface $\kappa = \sqrt{1 - s}$ and $s \in [0, 1]$

$$\tau_m(p) = \left( -\frac{1}{a_0} - ip + \mathcal{G}_m(p) \right)^{-1}$$
$$\kappa = \tanh \left( \frac{1}{\kappa} \left[ 1 - \frac{\pi}{2a_0 k_F} \right] \right), \quad \kappa \in [0, 1]$$



**Smooth transition** as a function of  $1/a_0 k_F$

**Cooper pairs** for  $1/(a_0 k_F) \rightarrow -\infty$

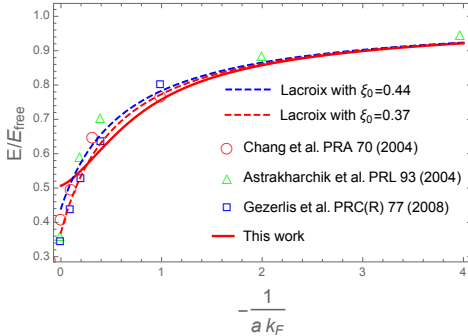
Total momentum,  $P = 2k_F s \rightarrow 0$ ,

and relative momentum

$$p = k_F \kappa \rightarrow k_F$$

**Unitary limit:**  $P = 2sk_F = 1.11k_F$   
and  $p = \kappa k_F = 0.88k_F$

**Molecular side:**  $2/\pi > a_0 k_F > 0$



**Lacroix:** Density functionals

**Rest:** Quantum Montecarlo [QM] calc.

## Including $r_0$ and $v_2$

$$v(k, p) = c_0 + \frac{1}{2}c_2(k^2 + p^2)$$

$$t_m(k, p) = \frac{4\pi/m}{-\frac{1}{a} + \frac{1}{2}r_0p^2 - ip + \mathcal{G}_m(p)}$$

## Including $r_0$ and $v_2$

$$\mathcal{E}_{\mathcal{L}} = \frac{8k_F^5}{m\pi^3} \int_0^1 ds s^2 \int_0^{\sqrt{1-s^2}} d\kappa \kappa \arctan \left( \frac{a_0 k_F I}{1 - a_0 r_0 k_F^2 \kappa^2 / 2 - a_0 k_F R / \pi} \right)$$

Bertsch parameter in the unitary limit  $\xi(r_0 k_F)$

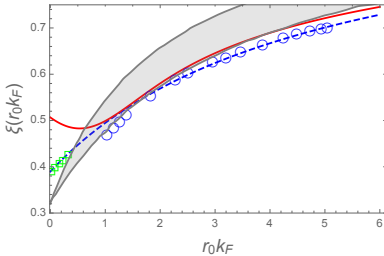
$$\xi(k_F) = 1 - \frac{80}{\pi} \int_0^1 ds s^2 \int_0^{\sqrt{1-s^2}} d\kappa \kappa \arctan \left( \frac{\pi I}{\pi r_0 k_F \kappa^2 / 2 + R} \right)$$

$$\xi(k_F) = \xi(r_0 = 0) + \eta_e r_0 k_F + \delta_e (r_0 k_F)^2 + \dots$$

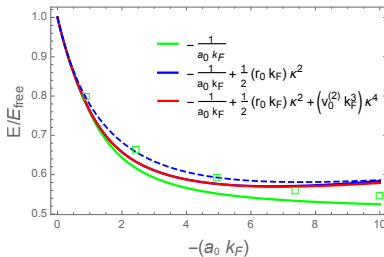
Our results [normal matter]:  $\eta_e = -0.0859$ ,  $\delta_e = 0.0644883$

QMC:  $\eta_e = 0.127$ ,  $\delta_e = -0.055$  Forbes, Gandolfi, Gezerlis'12

# Dependence of $\xi$ with $r_0$



**Blue dashed:** DFT Lacroix et al.'17  
**Circles:** Schwenk, Pethick'05  
**Squares:** QMC Forbes et al.'11; '12  
**Area:** Schäfer et al.'05



**Blue dashed:** DFT Lacroix'19  
**Squares:** QMC Gezerlis, Carlson'10

## Inclusion of $v_2$

$$v(k, p) = c_0 + c_2(k^2 + p^2) + c_4(k^4 + p^4)$$

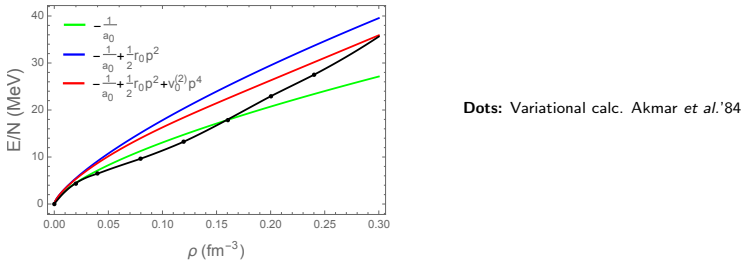
$$\mathcal{E}_L = \frac{8k_F^5}{m\pi^3} \int_0^1 ds s^2 \int_0^{\sqrt{1-s^2}} d\kappa \kappa \arctan \left( \frac{a_0 k_F I}{1 - a_0 r_0 k_F^2 \kappa^2 / 2 - a_0 v_0^{(2)} k_F^4 \kappa^4 - a_0 k_F R / \pi} \right)$$

$$\xi(k_F) = 1 - \frac{80}{\pi} \int_0^1 ds s^2 \int_0^{\sqrt{1-s^2}} d\kappa \kappa \arctan \left( \frac{I}{r_0 k_F \kappa^2 / 2 + v_0^{(2)} k_F^3 \kappa^4 + R / \pi} \right)$$

$$\xi(k_F) = \xi(r_0 = 0) + \eta_e r_0 k_F + \gamma_e v_0^{(2)} k_F^3 + \delta_e (r_0 k_F)^2 + \dots$$

Our result:  $\gamma_e = -0.164$

For neutron matter  $a_0 = -18.95 \pm 0.40$  fm Chen et al.'08,  $r_0 = 2.75$  fm  
and  $v_2 = -0.50$  fm<sup>3</sup> Navarro et al.'16

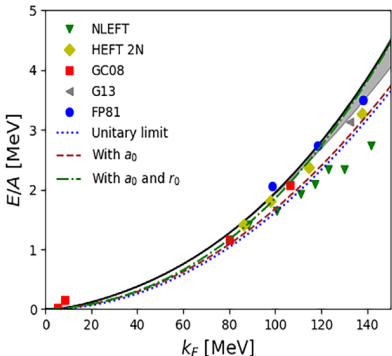


This curve was not well calculated algebraically until our work

It supports the Unitary-Gas Conjecture Tews et al.,  
Astrophys.J.848(2017)105

# Applications: Neutron matter [PNM]

- Our results for the resummation of ladder diagrams are renormalized
- $t_m$  and  $\bar{\mathcal{E}}$  are expressed directly in terms of experimental phase shifts and mixing angles
- We show them up to  $k_F \lesssim 150$  MeV. The off-shell part  $\propto q^\ell p^{\ell'}$  reflects the contact-interaction nature assumed as starting point. LC  $p^2 < -m_\pi^2/4$ .
- In density up to  $\rho \lesssim 1.5 \cdot 10^{-2} \text{ fm}^{-3} \approx 0.1 \rho_s$



Our results: Solid line

Unitary limit:  $a_0 \rightarrow \infty$ , dotted line

S-wave:  $a_0 = -18.95 \text{ fm}$ , dashed line

S-wave:  $a_0 + r_0 (= 2.75) \text{ fm}$ , dash-dotted line

NLEFT: NLO Chiral-EFT on the lattice Epelbaum et al.'09

FP81: Variational calculation Friedman, Pandharipande'81

G13: Auxiliary-Field QMC: N2LO  $\chi NN$  potential

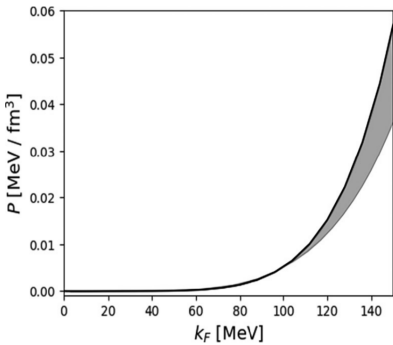
Gezerlis et al.'13

HEFT 2N: Auxiliary-Field QMC:  $V_{\text{low}-k}$  N3LO  $\chi NN$  potential Włazłowski et al.'14

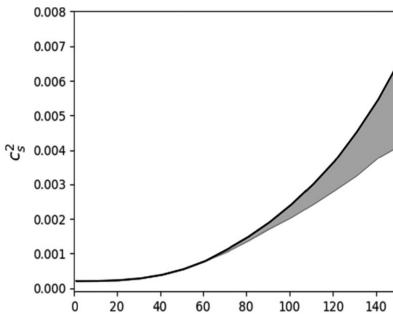
GC08: QMC calculations Gezerlis, Carlson'08

$P$ ,  $c_s^2$ ,  $S(\rho)$ ,  $L$

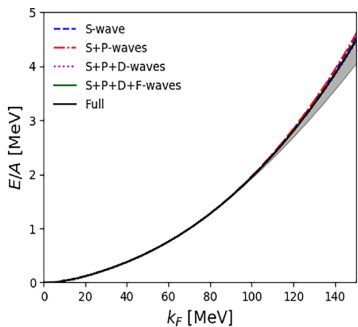
$$P(\rho) = \rho^2 \frac{\partial \bar{\mathcal{E}}}{\partial \rho}$$



$$\begin{aligned} c_s^2(\rho) &= \frac{1}{m} \frac{\partial P}{\partial \rho} \\ &= \frac{2\rho}{m} \frac{\partial \bar{\mathcal{E}}}{\partial \rho} + \frac{\rho^2}{m} \frac{\partial^2 \bar{\mathcal{E}}}{\partial \rho^2} \end{aligned}$$



# Partial-wave decomposition



It is dominated by the  $S$  wave—  
 $^1S_0$  PWA

Regulator:  $\exp(-(q - M_\pi/2)^2/\Lambda^2)$  for off-shell  $q > M_\pi/2$   
[entering in  $L_m$ ]

For  $k_F < 120$  MeV there is no significant impact for  $\Lambda \gtrsim M_\pi$

Its effect increases for higher  $k_F$ , as expected

**Symmetry energy:**  $S(\rho) = \bar{\mathcal{E}}_{\text{PNM}}(\rho) - \bar{\mathcal{E}}_{\text{SNM}}(\rho)$

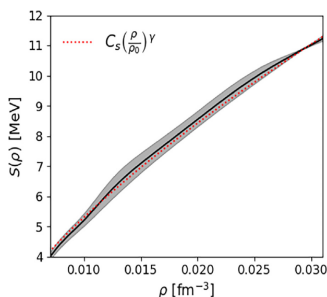
$$\textcolor{blue}{L} \text{ Slope of } S(\rho) \text{ at } \rho_0 \quad L = 3\rho_0 \left. \frac{dS(\rho)}{d\rho} \right|_{\rho_0}$$

**Fit:**  $S_0$ ,  $\textcolor{blue}{L}$  Simple parameterization

$$\bar{\mathcal{E}}(\rho, x_p), x_p \equiv \rho_p/\rho \quad \text{Gandolfi et al.'18}$$

$$\bar{\mathcal{E}}(\rho, x_p) = \bar{\mathcal{E}}(\rho, \frac{1}{2}) + C_s \left( \frac{\rho}{\rho_0} \right)^{\gamma_s} (1 - 2x_p)^2$$

$$L = 3C_s \gamma_s$$

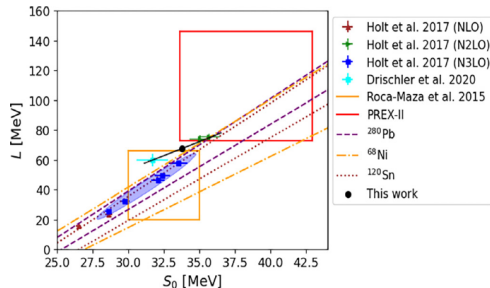


Fit:  $C_s = 34.77 \pm 0.15 \text{ MeV}$ ,

$$\gamma_s = 0.667 \pm 0.003$$

Empirical bands extracted from static dipole polarizability in nuclei  
 $^{280}\text{Pb}$ ,  $^{68}\text{Ni}$ ,  $^{120}\text{Sn}$  Roca-Maza et al.'15

Perturbative  $\chi$ -EFT at NLO,N2LO,N3LO Holt,Kaiser'17



Correlation ellipse at 95% C.L.

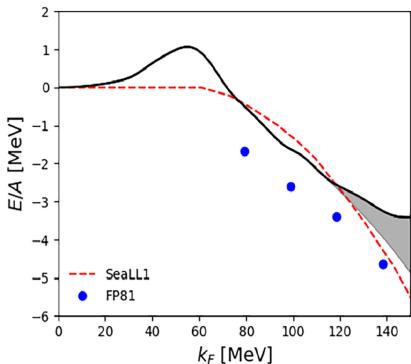
$$31 \text{ MeV} < S_0 < 38 \text{ MeV}$$

$$57 \text{ MeV} < L < 84 \text{ MeV}$$

# Symmetric Nuclear Matter [SNM]

Alarcón, JAO, forthcoming

- Up to  $k_F < 150$  MeV or  $\rho = 3 \cdot 10^{-2}$  fm $^{-3}$



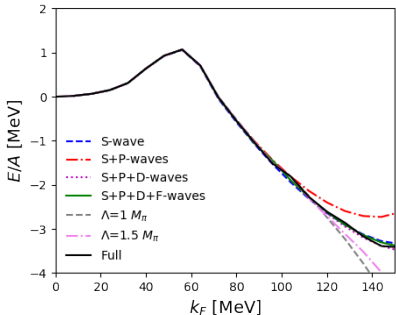
FP81: MC variational calc. Friedman, Pandharipande'91

SeaLL1: Density Functional calc. Bulgac *et al.*'18

## Spinodal instability

$\tilde{\mathcal{E}} > 0$  up to  $k_F < 70$  MeV. SNM is no the most favorable phase,  $\alpha$  and heavy nuclei form Shen *et al.*'98

# Partial-wave decomposition



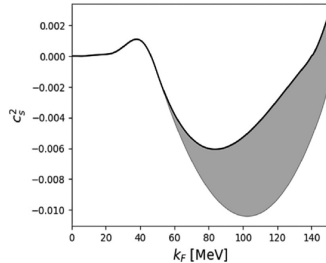
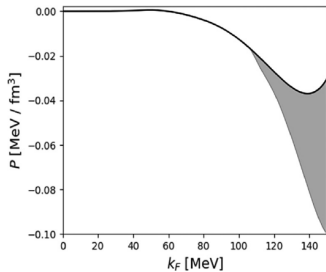
Dominance of  $S$ -waves  
 $P$ -wave contribution is repulsive,  
but cancelled by higher waves

Regulator:  $\exp(-(q - M_\pi/2)^2/\Lambda^2)$  for off-shell  $q > M_\pi/2$   
[entering in  $L_m$ ]

For  $k_F < 120$  MeV there is not impact on  $\Lambda \gtrsim M_\pi$

It keeps growing for  $k_F > 120$  MeV, as expected

## $P$ and $c_s^2$



$P > 0$  up to  $k_F = 59$  MeV

$c_s^2 < 0$  up to  $k_F = \xi_c = 140$  MeV or  $\rho = 2.4 \cdot 10^{-2}$  fm<sup>-3</sup>   [ $K = \frac{c_s^2}{m\rho}$ ]

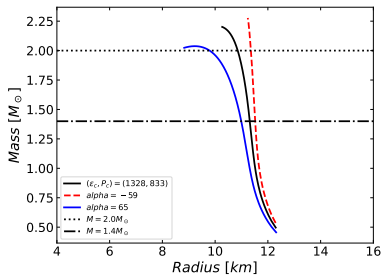
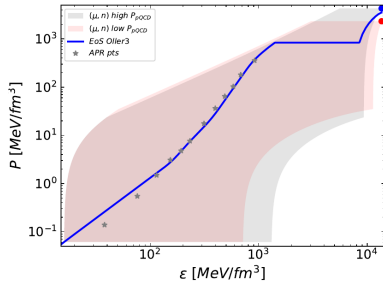
$\xi_c \approx 190$  MeV [Shen et al.'98](#) and  $\xi_c \approx 200$  MeV [Machleidt et al.](#)

## Conclusions

- ① The ladder diagrams to calculate  $\bar{\mathcal{E}} \equiv E/A$  is resummed
- ② This is done for arbitrary vacuum fermion-fermion interactions
- ③ And also for arbitrary regularization method
- ④ The case of contact interactions is fully solved for arbitrary cutoff regularization
- ⑤ DR regularization is disregarded [for finite order ERE]
- ⑥ Renormalized  $\bar{\mathcal{E}}$  is obtained and expressed in terms of experimental scattering data. No free parameters, no scale dependence.

- ⑧ Application to  $S$  waves: Including  $a_0$ ,  $r_0$ ,  $v_2$
- ⑨ PNM and SNM are studied for  $k_F < 150$  MeV
- ⑩  $\bar{\mathcal{E}}$ ,  $P$ ,  $c_s^2$ ,  $K$ ,  $S(\rho)$ ,  $S_0$  and  $L$  are provided
- ⑪ Restrict EOS parameterizations for low  $\rho$
- ⑫ Then, extrapolate these results to larger  $\rho$

From Eva Lope Oter's talk



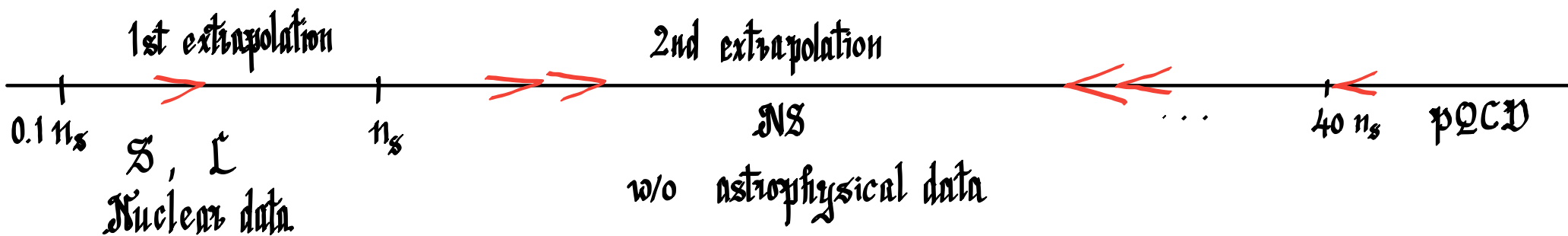
NICER's constraint  $R = 11.8 - 13.1$  Km at  $1.4M_\odot$  Kostas  
Glampedakis' talk

## Extrapolation to higher densities of the EoS OLA Alarcón, JAO, PRC 107 (2023)

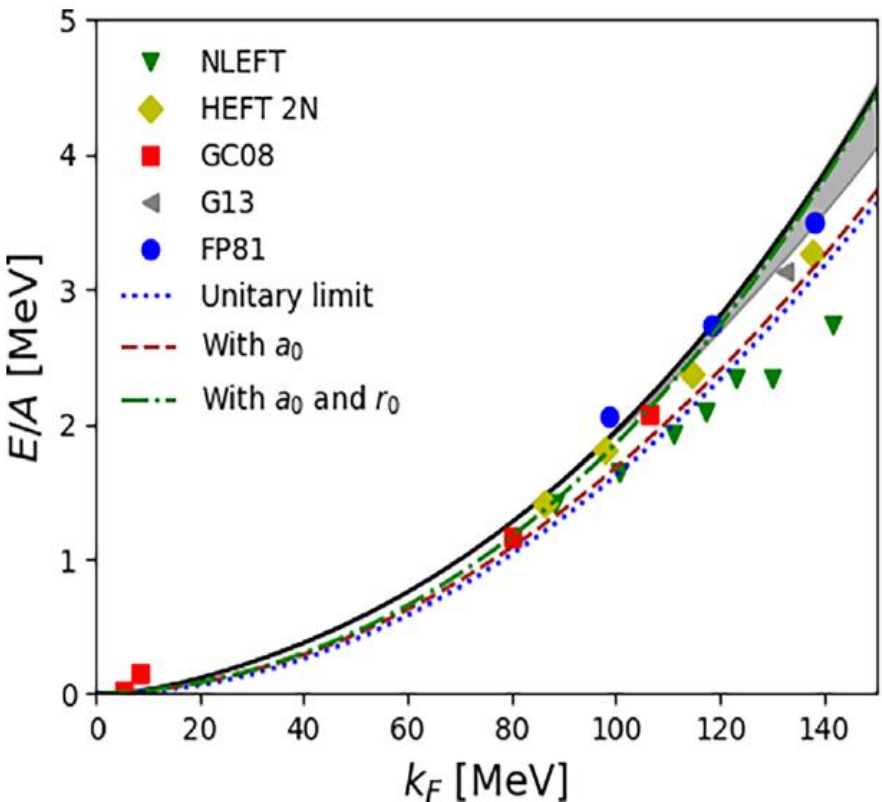
From  $n \approx 0.1 n_s$  up to  $\text{pQCD}$   $n \sim 45 n_s$ ,  $n_s = 0.16 \text{ fm}^{-3}$

NLO  $\text{pQCD}$  Gorda et al, PRL 127 (2021)  
 $O(\alpha_s^3)$

In between we have the NS density region  $n_{c,\max} \approx 6.5 n_s$



## OIA EoS



3. Was solved for contact interactions,  $k_F \leq 150$  MeV

1. Renormalized  
No regulator dependence

2. Directly expressed  
in terms of experimental  
data,  $\delta(2s+1L_J)$ ,  $\epsilon_{L-L'}$

3. Specific in-medium  
power counting.  
LO calculation  $\rightarrow$  Ladder  
Resummation

Nonperturbative calculation  
 $\delta_1 - \delta_1$ : Deuterion  
 $\delta_0 - \delta_0$ : Antibound state

Many-body perturbation  
calculations in chiral EFT

1. Strong cutoff dependence

Small variation 450-500 MeV  
- 10% -

2. A potential with many  
free parameters fitted  
to data is required  
intrinsic difficulties

3. Naive use of vacuum  
power counting

They neglect this  
and show results only  
for  $\eta > 0.5 \eta_S$

The upper limit  $n = 0.1 n_s$  in OLA is in the crust region

$E/A$  relative to uniform nuclear matter in  $\beta$  equilibrium ( $npe$ ) Sharma et al. A&A 584 (2015)

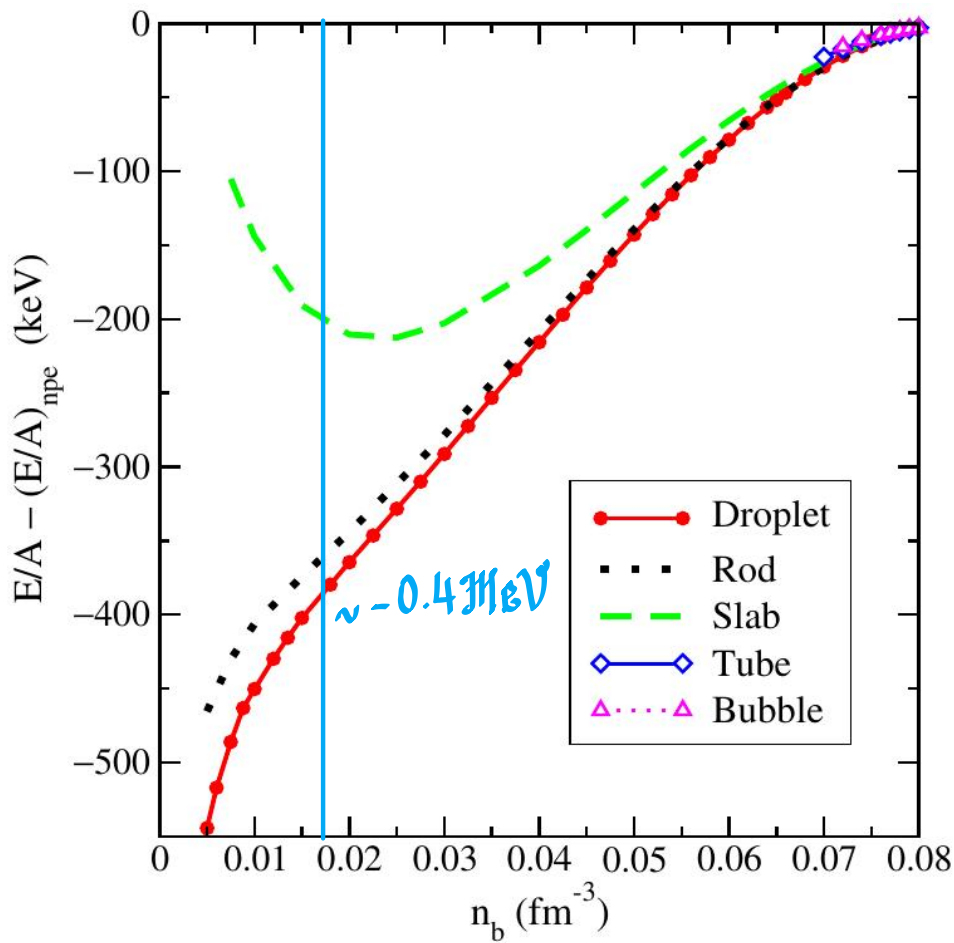
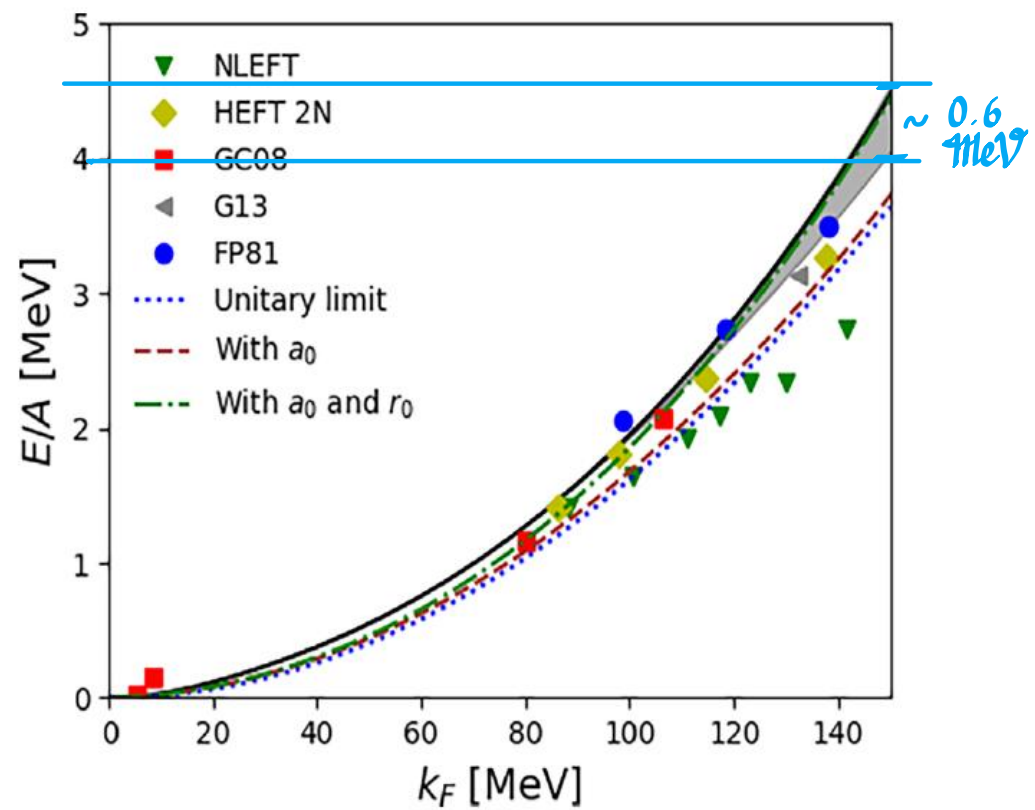


**Fig. 3.** Energy per baryon of different shapes relative to uniform  $npe$  matter as a function of baryon density in the inner crust.



It is perfectly inside our uncertainty band.  
Proton fraction < 3%.

## Extrapolation method based on Lope Oter et al., JFM 46 (2019) Komolgov, Kurkela, PRL 128 (2022)

We mostly proceed in the  $(\xi, \eta)$  plane  
and to a lesser extent in the  $(\mu, n)$  plane

$$\xi = \frac{n}{N} \quad n = \frac{N}{V}$$

Lowest density part :  $\text{OLA} : \text{ELA}(n)$

Back and forth from different along trajectories of extrapolation planes

$$\xi = n(M_N + E/A)$$

$$\eta^2 = n^2 \frac{d(E/A)}{dn}$$

And viceversa.  
Discretizing

$$n_{i+1} = \frac{\xi_{i+1}}{M_N + (E/A)_{i-1}} \quad \left. \begin{array}{l} E/A_{i+1} \\ n_{i+1} \end{array} \right\}$$

$$\eta_i = \eta_i^2 \frac{(E/A)_{i+1} - (E/A)_{i-1}}{n_{i+1} - n_{i-1}}$$

known  
at  $i, i-1$

$$\mu_i = \frac{\xi_i + \eta_i}{n_i} \text{ Euler equation}$$

In the extrapolation the causality conditions are fulfilled

$$(\xi, \eta) \text{ plane: } c_s^2 = \frac{d\eta(\xi)}{d\xi} \quad \boxed{0 \leq c_s^2 \leq 1}$$

This delimits an area in  $(\xi, \eta)$  plane between the extremes in the extrapolation. A  $10^3 \times 10^3$  grid is constructed.

$$(\mu, n) \text{ plane: } c_s^{-2} = \frac{\mu}{n} \frac{dn(\mu)}{d\mu} \quad \boxed{c_s^2 \geq 1}$$

Simultaneously with the  $(\xi, \eta)$  causal constraint.

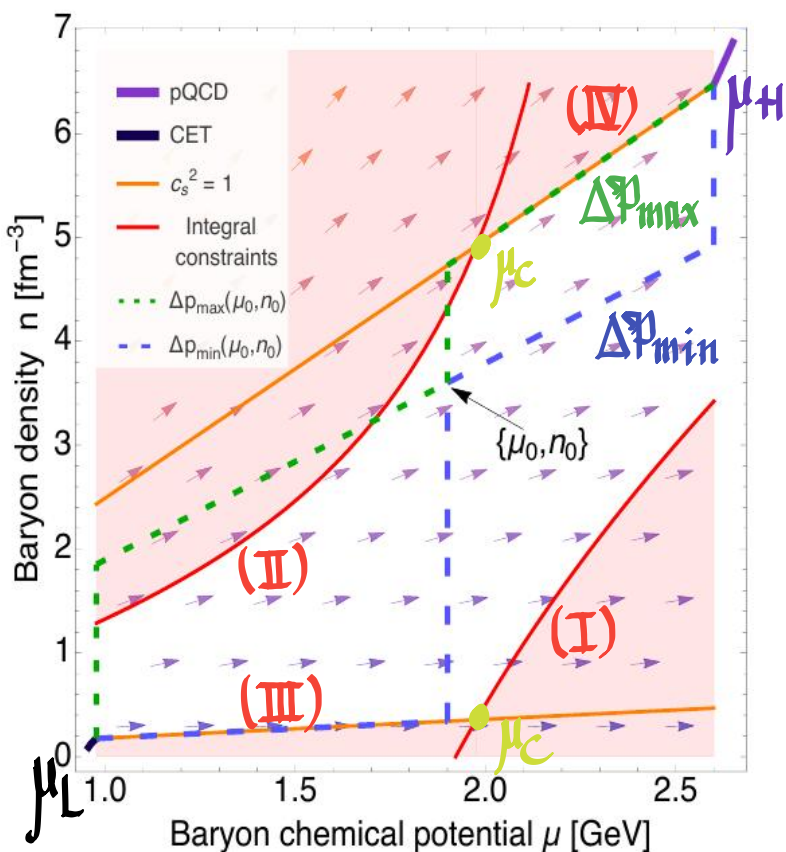
The causal area is further limited by

$$\frac{d\mathfrak{P}(\mu)}{d\mu} = n(\mu) \rightarrow \mathfrak{P}_H - \mathfrak{P}(n) = \int_{\mu(n)}^{\mu_H} d\mu \, n(\mu)$$

This result and

$$c_s^{-2} = \frac{\mu}{n} \frac{dn(\mu)}{d\mu} \geq 1 \rightarrow \frac{dn(\mu)}{d\mu} \geq \frac{n}{\mu}$$

are heavily used by Komatsu and Kukela  
PLB 128 (2022)

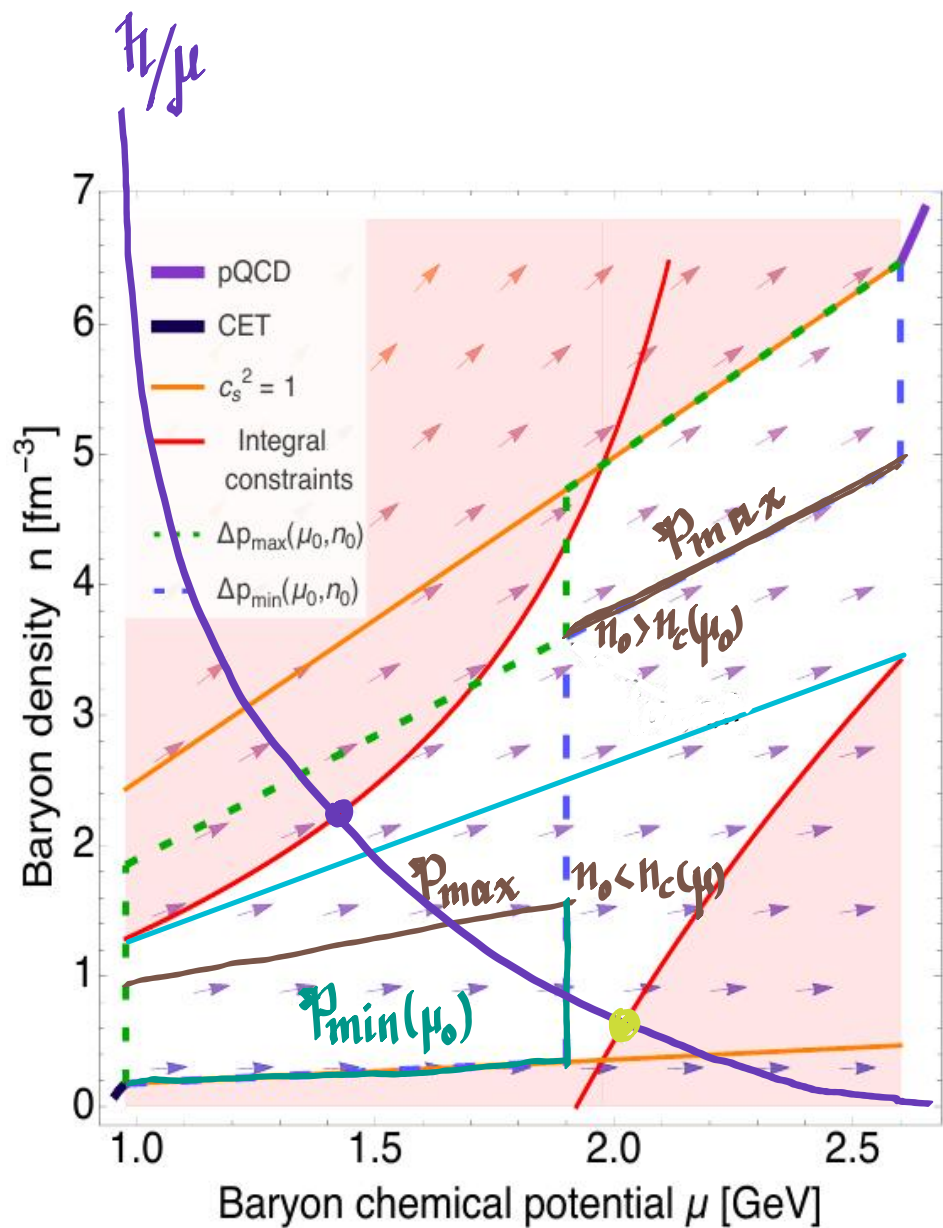


$$\Delta \mathfrak{P}_{\max} = \mathfrak{P}_H - \mathfrak{P}_L = \Delta \mathfrak{P}_{\min} \quad (\text{I}) \quad (\text{II})$$

$$\frac{dn(\mu)}{d\mu} = \frac{n}{\mu} \quad (\text{III}), (\text{IV})$$

$$\mu_c = \sqrt{\frac{\mu_L \mu_H (\mu_H n_H - \mu_L n_L - 2\Delta p)}{\mu_L n_H - \mu_H n_L}}$$

This construction in the  $(\mu, n)$  is taken to the  $(\varepsilon, \beta)$  plane  
by using the Euler equation



$$\varepsilon = -\beta + \mu n$$

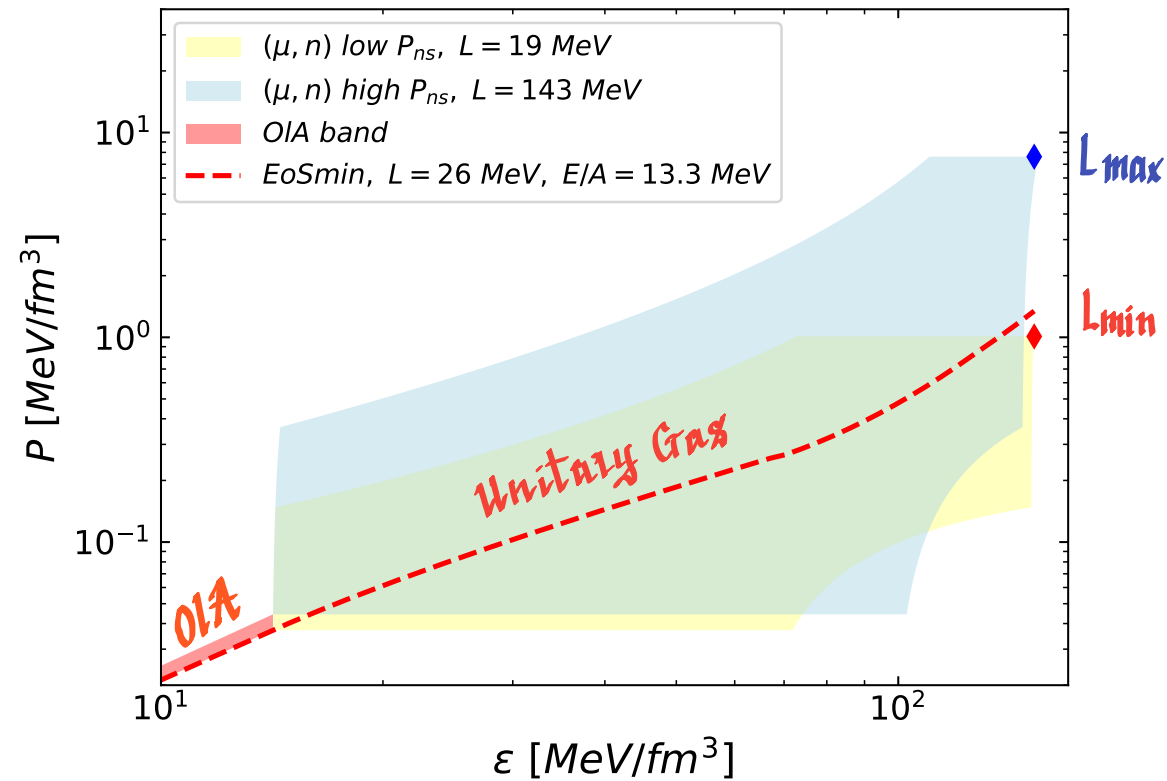
1. Determine  $\beta_{\min}(\mu_0, n_0)$ ,  $\beta_{\max}(\mu_0, n_0)$   
at each allowed  $(n_0, \mu_0)$
2. Fixed-bimetric lines  $\beta = \varepsilon + \beta = \mu n$

$$(\varepsilon, \beta) : \beta(\varepsilon) = h - \varepsilon \\ (\mu, n) : n(\mu) = \frac{h}{\mu}$$

$\beta$  is maximized/minimized along  
the same isenthalpic line in both planes

- $\{\varepsilon_{\max}(\mu), \beta_{\min}(\mu)\}$   
Lower boundary in  $(\varepsilon, \beta)$  plane
- $\{\varepsilon_{\min}(\mu), \beta_{\max}(\mu)\}$   
Upper Boundary in  $(\varepsilon, \beta)$  plane

Extrapolation:  $0.1 n_s \leq n \leq n_s$   
of Ola EoS



$$\mu_s = M_N + \left. \frac{E}{A} \right|_s + \frac{p_s}{n_s} \quad \text{Needed for the construction}$$

in the  $(\mu, n)$  plane  $H=8$

$$\blacklozenge p_s = 7.6 \text{ MeV fm}^{-3}, \mu_s = 1013.5 \text{ MeV}$$

$$\blacklozenge p_s = 1.0 \text{ MeV fm}^{-3}, \mu_s = 962 \text{ MeV}$$

Experimental Information:

$$\left. \begin{array}{l} \frac{E}{A} \\ p \end{array} \right|_{SNM} = -16.0 \pm 0.5 \text{ MeV} \quad \left. \begin{array}{l} n_s \\ p \end{array} \right|_{SNM} = 0.16 \pm 0.01 \text{ fm}^{-3} \quad \left. \begin{array}{l} \text{Beender, Heenen,} \\ \text{Reinhard,} \\ \text{KMP 75 (2005)} \end{array} \right\}$$

$$S_0 = \left. \frac{E}{A} \right|_{PNM} (n_s) - \left. \frac{E}{A} \right|_{SNM} (n_s)$$

$$L = 3n_s \frac{dp}{dn} S(n) \Big|_{n_s} = \frac{3}{n_s} p(n_s)$$

PREX II Reed et al. PRL 126 (2021)

$$S_0 = 38.1 \pm 4.7 \text{ MeV}$$

$$L = 106 \pm 37 \text{ MeV}$$

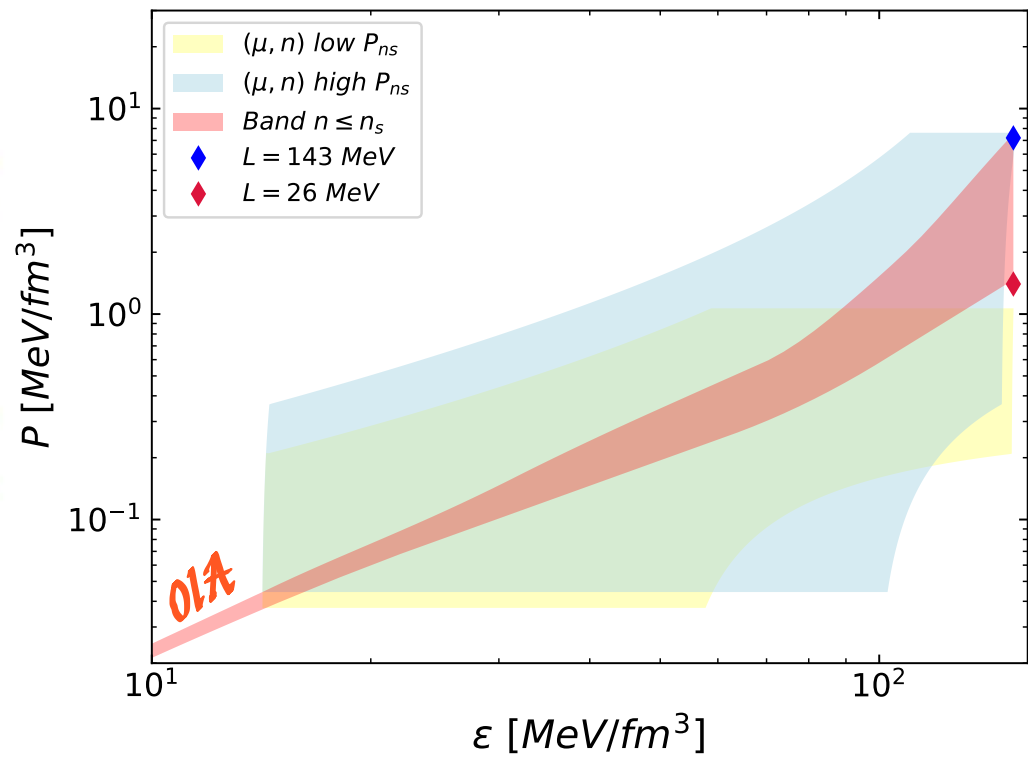
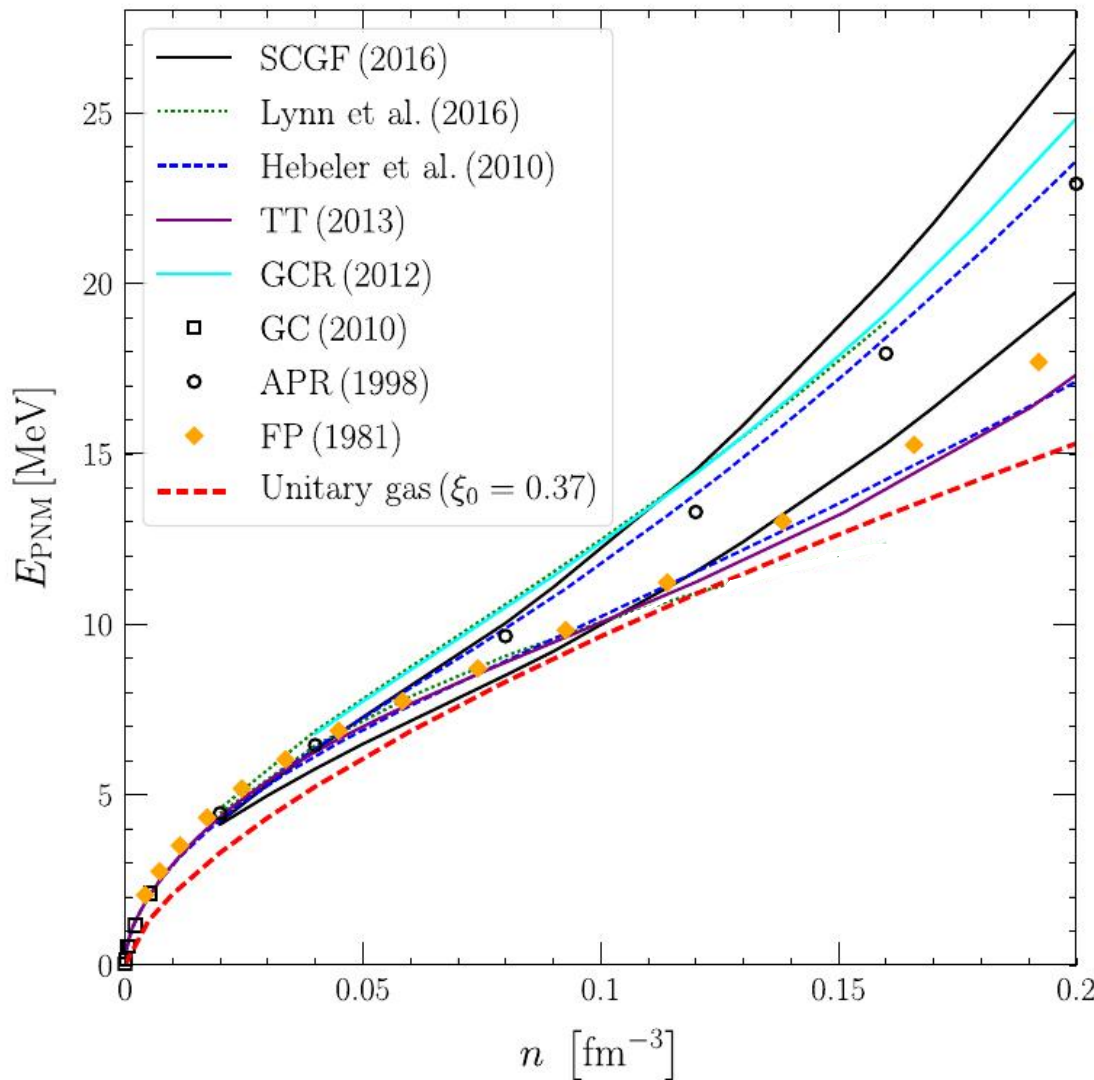
CREX Reed et al. PRC 109 (2024)

$$1. - L = 110 \pm 40 \text{ MeV}$$

$$2. - L = 19 \pm 19 \text{ MeV}$$

Instead of the controversial minimum value for  $\mathcal{L}$  we limit  $p_s$  by using the Unitary Gas Conjecture (UGC) : Unitary gas sets a lower bound on  $E/A$

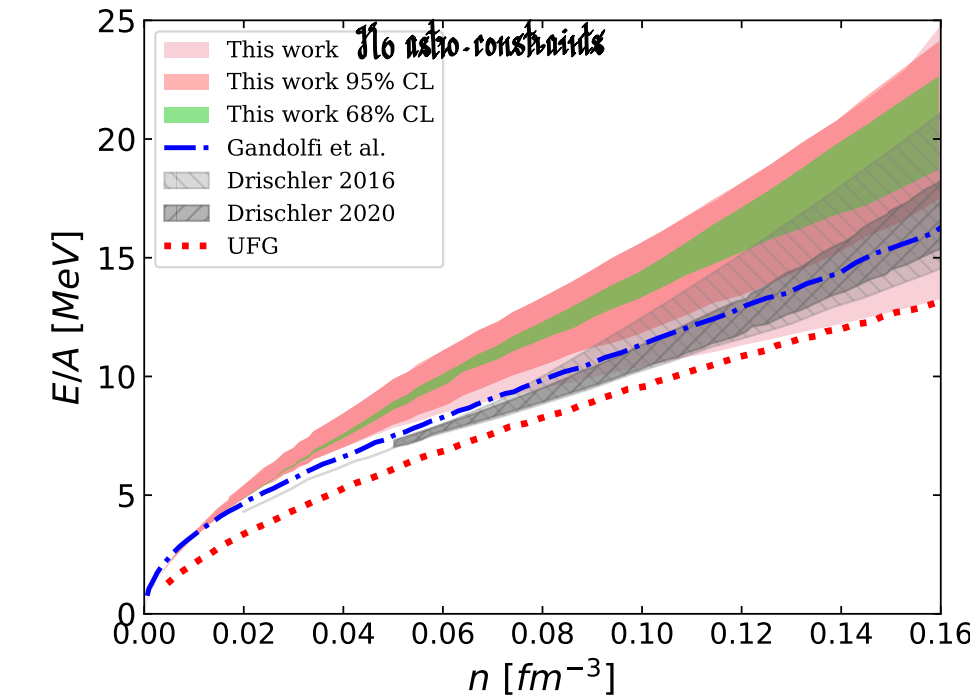
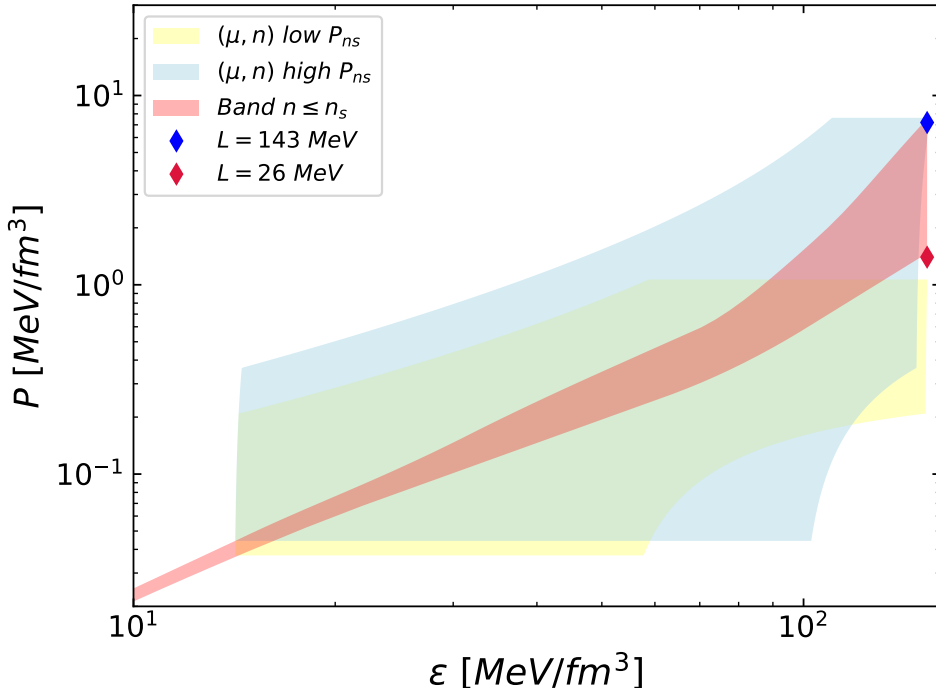
Tews et al. *Astrophys. J.* 848 (2017)



$$\left. \begin{array}{l} p_s = 1.4 \text{ MeV fm}^{-3} \\ \mathcal{L} = 26 \text{ MeV} \end{array} \right\} \text{UGC}$$

$$E/A = 16.9 \text{ MeV} \quad \text{CREX+SNM}$$

$$E/A|_{\text{UGC}} = 13.2 \text{ MeV}$$



$$\uparrow \rho_s = 7.62 \text{ fm}^{-3}$$

$$\downarrow \rho_s = 1.41 \text{ fm}^{-3}$$

In the grid: proceed from lower to higher densities.

$c_s^2$  from point to point raises softly  
with  $dc_s^2/d\varepsilon > 0$

Avoid too early phase transitions

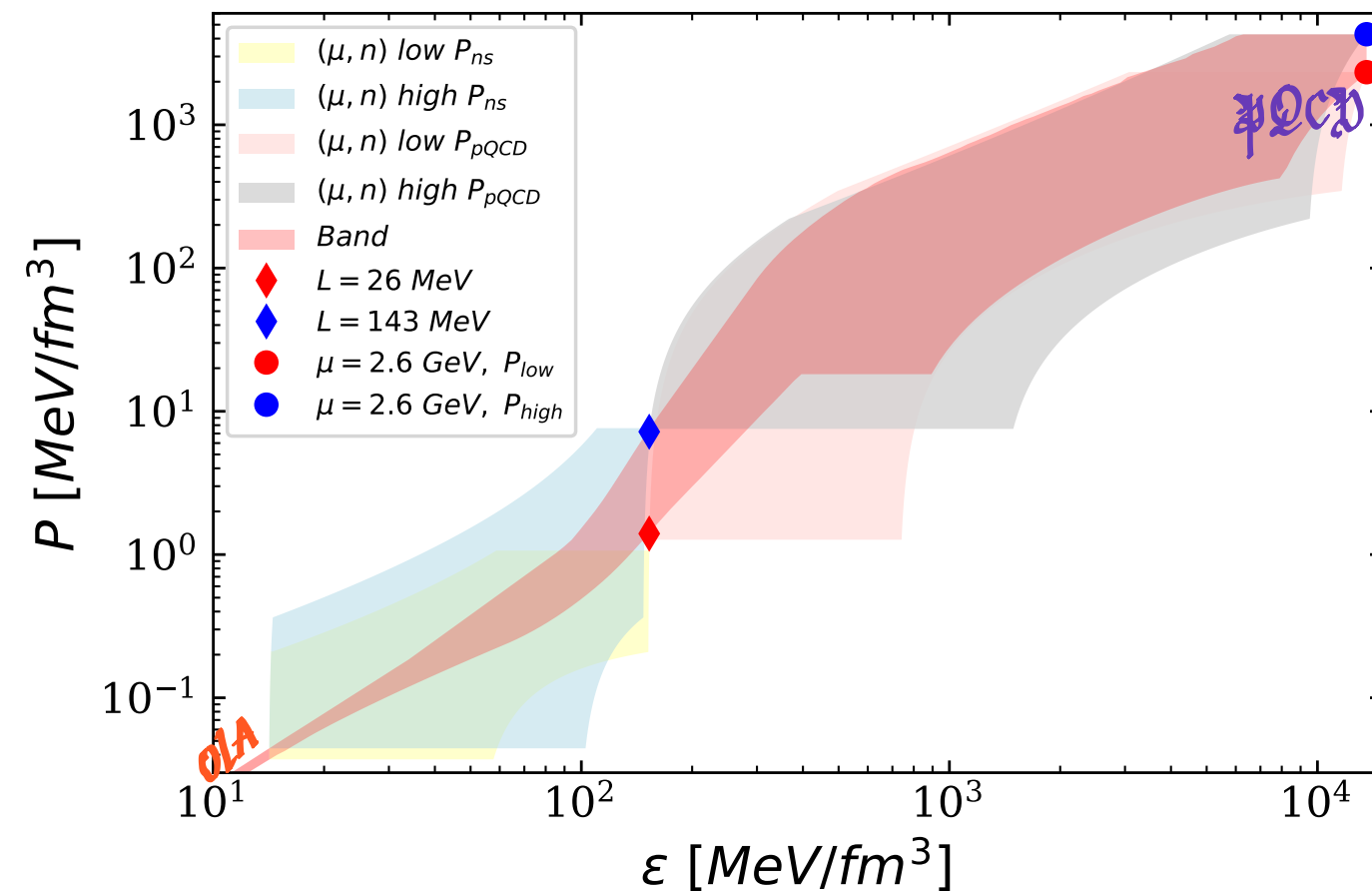
Our values taken as input from phenomenology and UFC

$$30.5 \leq s \leq 43.5 \text{ MeV}$$

$$26.5 \leq L \leq 143 \text{ MeV}$$

Extrapolation from  $\eta_s$  up to  $\mu_{QCD} \approx 40 \eta_s$

Highest density region from  $N^3LO$   $\mu_{QCD}$   $\beta(\mu)$   
Gorda et al. PRD 104 ('21)



$$\mu_H = 2.6 \text{ GeV}$$

$$\left. \begin{array}{l} 4384 \\ 2334 \end{array} \right\} \rightarrow \chi \in [1, 4]$$

Renormalization scale

$$\chi = \frac{3\Lambda}{\mu}$$

$$\eta_s < \eta < 2.5 \eta_s$$

$c_s^2$  softly increases

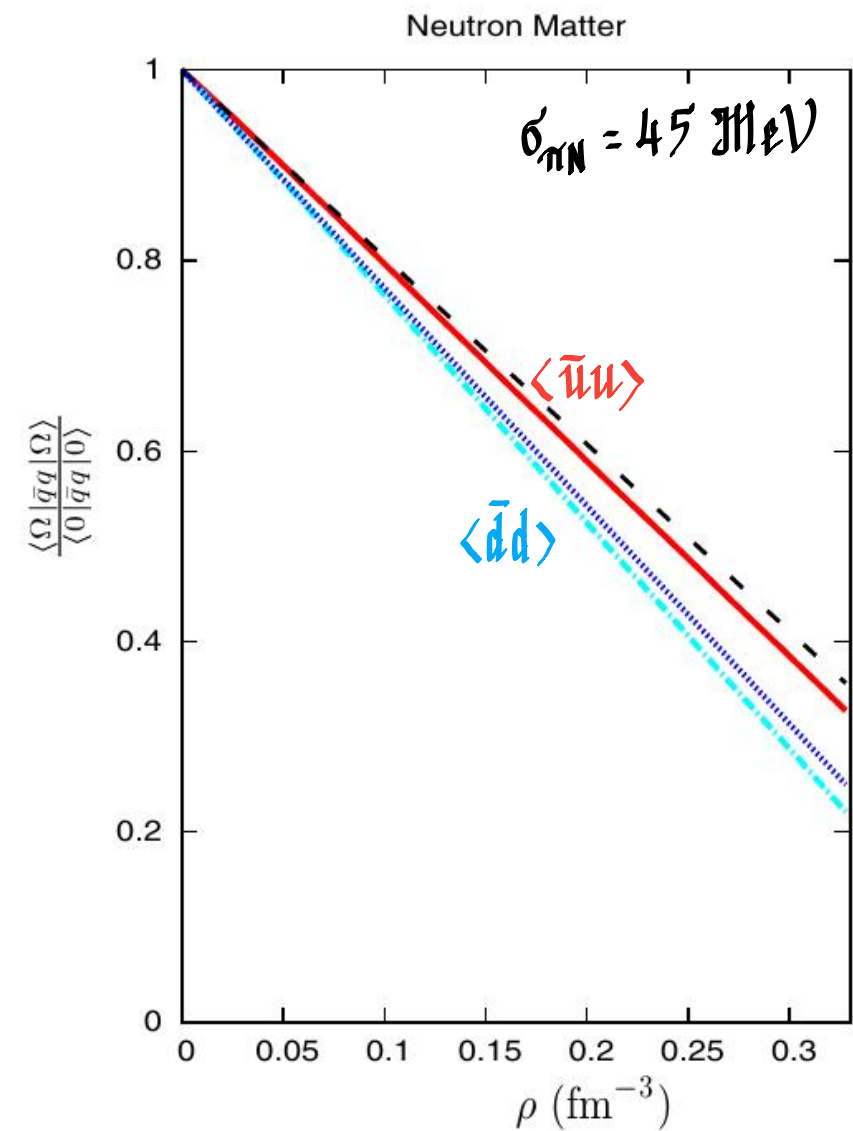
$$\frac{dc_s^2}{d\eta} > 0$$

$$\eta > 2.5 \eta_s$$

Phase transitions (PT)  
are allowed

Why?

Because of the behavior of the quark condensate  $\langle \Omega | \bar{q} q | \Omega \rangle$  (ii)



Vanishing almost linearly in  $\sigma_{\pi N}$

2.5 ns for  $\sigma_{\pi N} \approx 50 \text{ MeV}$

Largest  $\sigma_{\pi N} \approx 60 \text{ MeV}$

Alarcon et al. *PRD* 85 ('10)  
Hofenrichter et al. *PRL* 115 ('15)

Chiral EFT  
Dispersion relations  
Exp data  $\pi N$

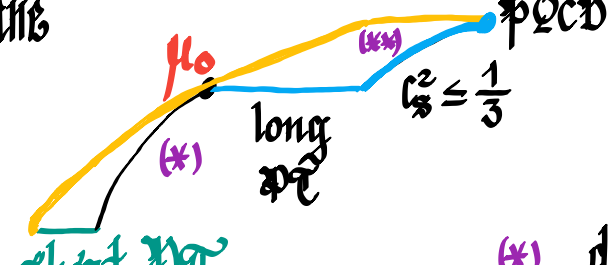
Lattice QCD: Smaller values  
 $43.7 \pm 3.6 \text{ MeV}$

Agadjanov et al. *PRL* 131 ('23)

$$n > 2.5 n_s$$

$\frac{dc_s^2}{d\epsilon} \geq 0$  i.e.  $\frac{dc_s^2}{d\epsilon} = 0$  is allowed ; Jump in  $\epsilon$  with  $p = ct$   
 $c_s^2 = 0$  along PT

( $\epsilon, p$ ) plane



[Not in all EoS]  
Only for  $M_{NS} \geq 2.18 M_\odot$

Brandes, Weise Symmetry 16('24)

statistical analysis  
conclude against PT  
 $M_{NS} \leq 2.1 M_\odot$

(\*)  $\frac{dc_s^2}{d\epsilon} > 0$  smooth rising  
until  $c_s = c_{s,\max}$

(\*\*) Highest density  
Practical realization showing  
explicit compatibility with pQCD

$$c_{s,\max}^2 = 1$$

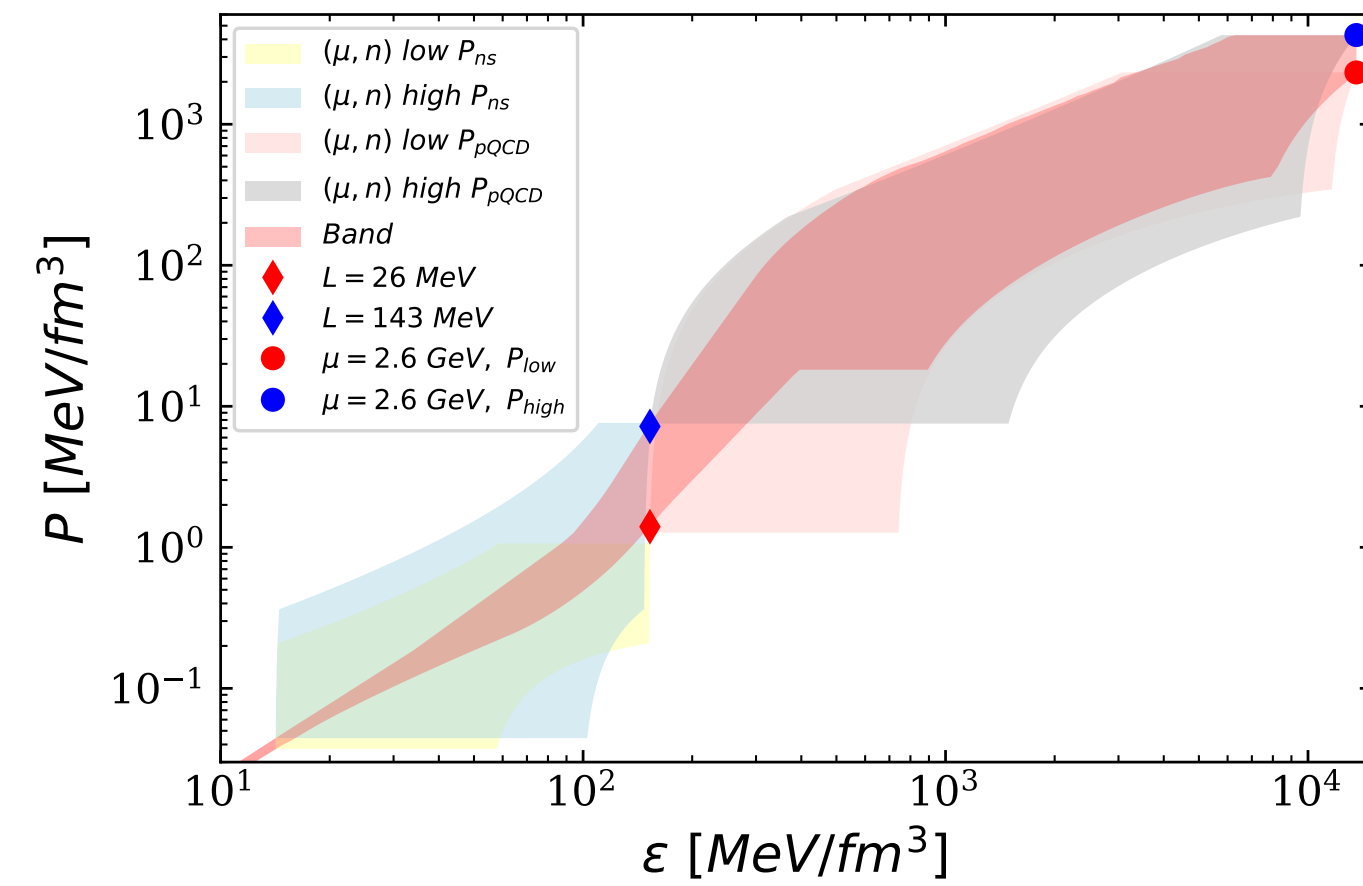
$$\mu_0 = 2250 \text{ MeV} < \mu_c \approx 2500 \text{ MeV}$$

$$c_{s,\max}^2 = 0.781$$

$$\mu_0 = 2040 \text{ MeV}$$

Hippert et al., 2402.14085  
Lang et al., 2404.09563

$\approx$  Central neutron star  
density



Constrained by

Causality

Thermodynamical consistency

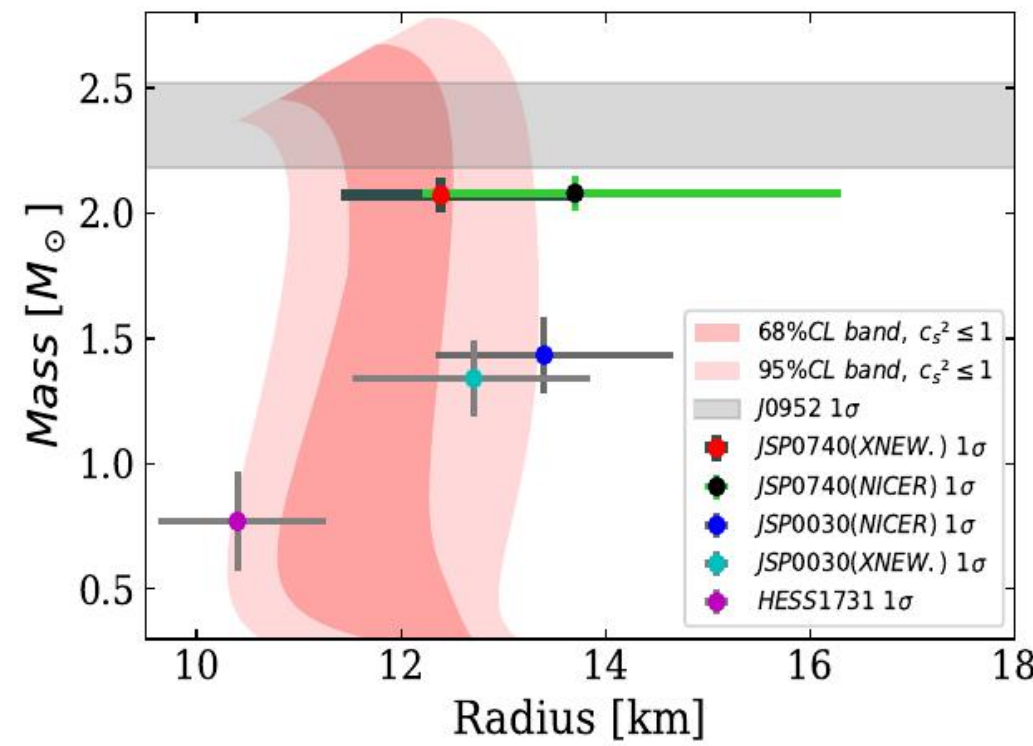
Thermodynamical stability

pQCD

Empirical nuclear data

No astrophysical constraints

Astrophysical constraints included and calculated with GR.  
 6 NS masses, 5 radii, 3 tidal deformabilities. Augmented TOV system of equations  
 are solved



$$5.0 n_g \leq n_{c,\max} \leq 6.1 n_g$$

$$2230 \leq \mu_{c,\max} \leq 2240 \text{ MeV}$$

$\Phi T$ s for  $M > 2.18 M_\odot$

$$3.2 n_g \leq n_c \leq n_{c,\max}$$

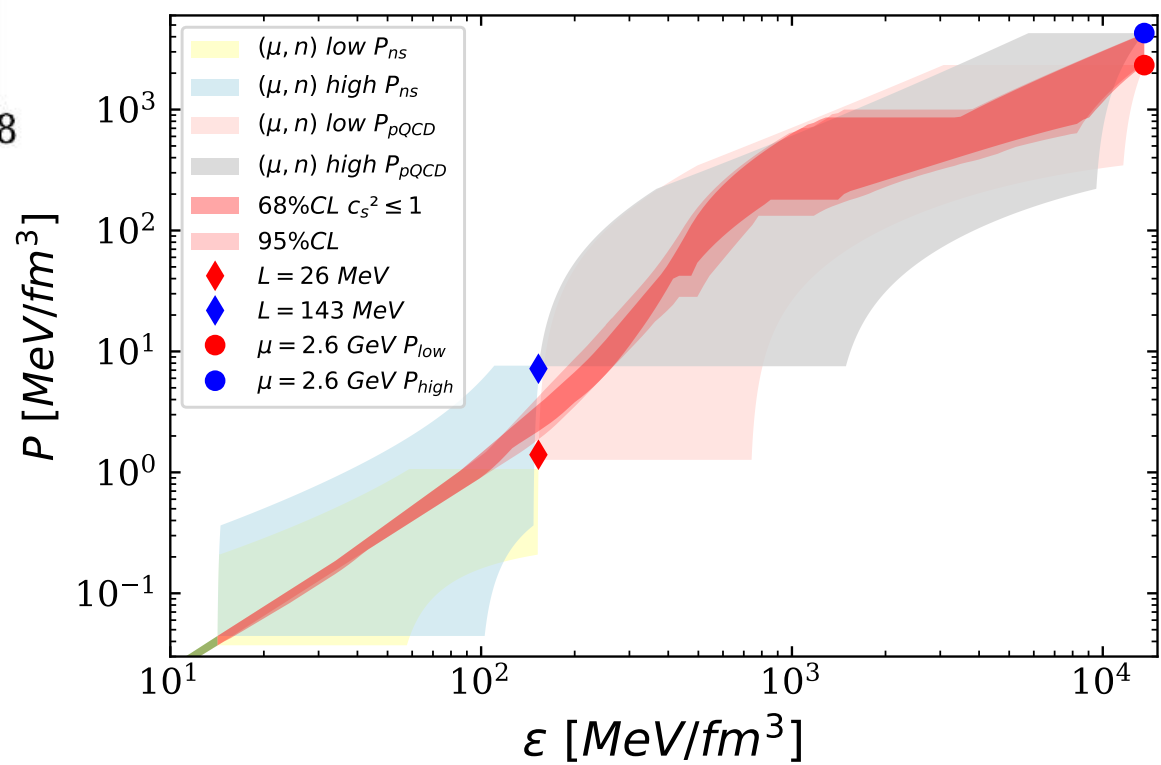
1st order  $\Phi T$   $\Delta n/n > 1$

$$c_s^2 \leq 1$$

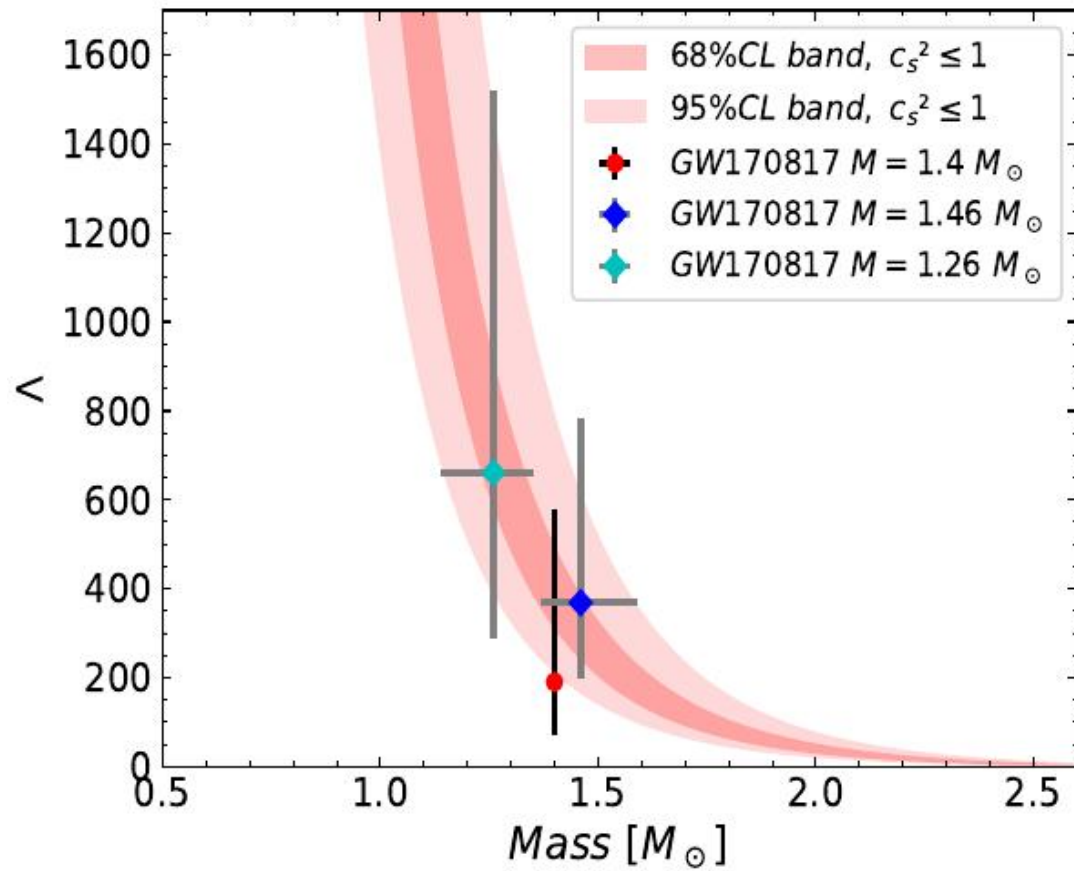
$\delta_0, L$  are further restricted

$$35.9 \leq \delta_0 \leq 39.7 \text{ MeV}$$

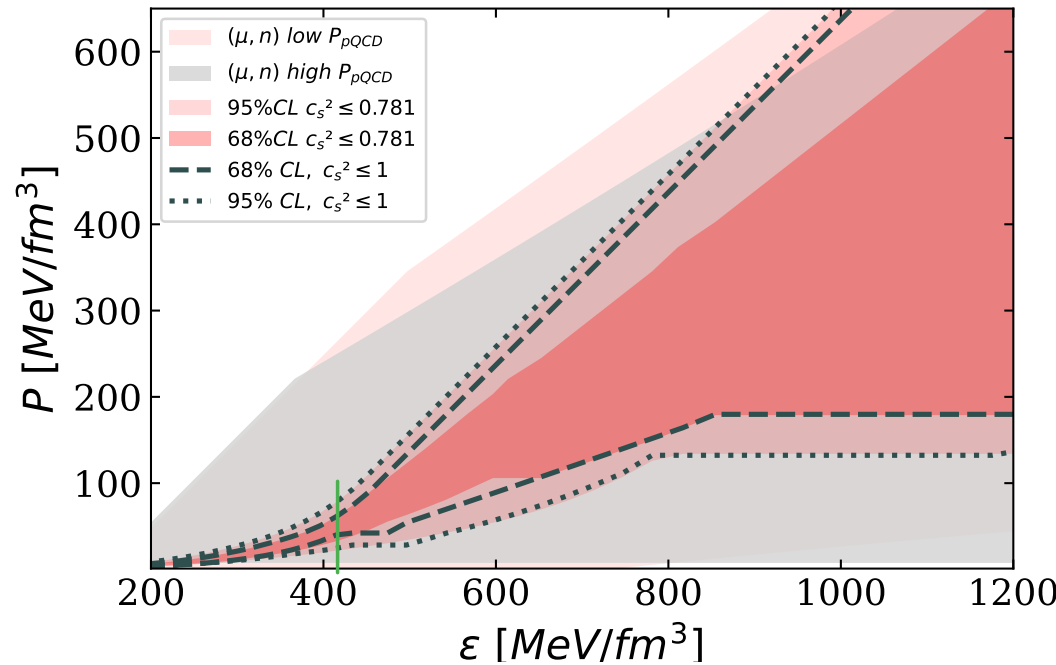
$$41.0 \leq L \leq 68.0 \text{ MeV}$$



# Tidal Deformability



Upper limit:  $c_s^2 \leq 0.781$  Hippel et al., 2402.14085 ; Tang et al., 2404.09563



$\varepsilon \lesssim 450 \text{ MeV fm}^{-3}$

The same band  
as with  $c_s^2 \leq 1$

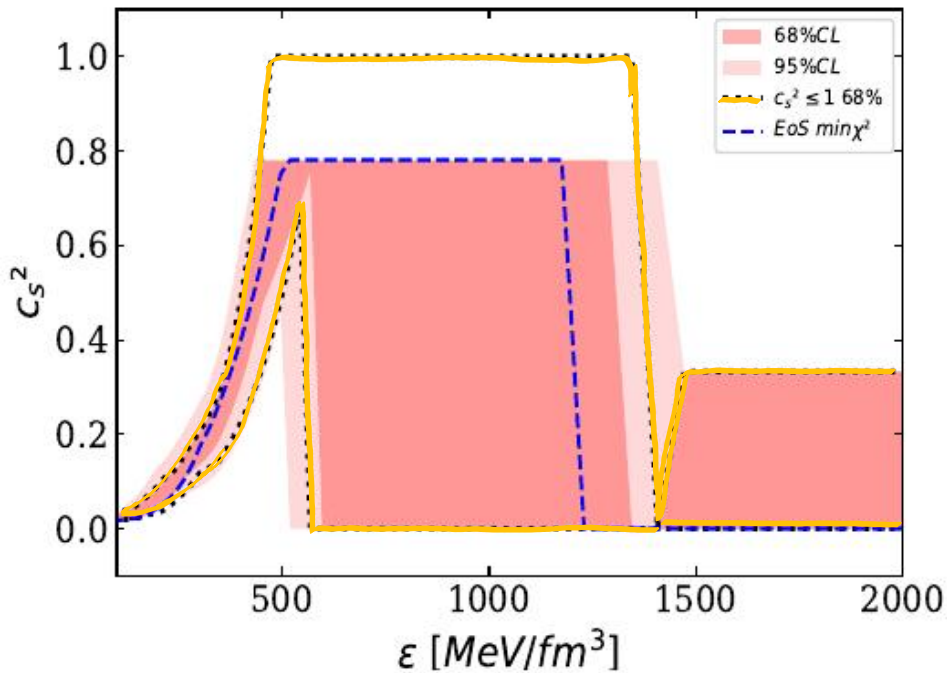
Larger  $5.2 n_s \leq n_{c,\max} \leq 6.52 n_s$

Smaller  $\mu_{c,\max} \approx 2020 \text{ MeV}$

$\mathfrak{PT}_s M \geq 2.18 M_\odot$ ,  $3.3 n_s \leq n \leq n_{c,\max}$

1st order  $\mathfrak{PT}$   $\Delta n/n > 1$

# Speed of sound squared



## Conclusions

- 1.- Renormalized and cutoff independent EoS for nuclear matter,  $n \leq 0.1 n_s$   
 $k_F \lesssim m_\pi \approx \frac{k_{F,s}}{2}$
- 2.- By resumming the ladder series, LO in-medium corrections  
already a nonperturbative calculation
- 3.- Directly expressed in terms of  
nucleon-nucleon scattering data.
4. Extrapolation until  $n_s$ ,  $n_{c,\max}$ ,  $\mathcal{PTC}$   
causality, Thermodynamical consistency and stability ( $\mu, n$ ), ( $\epsilon, P$ ) planes  
 $\mathcal{PTC}$ , Nuclear and Astrophysical data
5.  $35.9 \leq S_0 \leq 39.7 \text{ MeV}$        $5.0 n_s \leq n_{c,\max} \leq 6.1 n_s$   
 $41.0 \leq L \leq 68.0 \text{ MeV}$        $2230 \leq \mu_{c,\max} \leq 2240 \text{ MeV}$   
 $\mathcal{PT}$ s for  $M > 2.18 M_\odot$   
 $3.2 n_s \leq n_c \leq n_{c,\max}$   
1st order  $\mathcal{PT}$   $\Delta n/n > 1$